processes

MDPI

Article

Research on Erosion Wear of Slotted Screen Based on High Production Gas Field

Fucheng Deng [1,2,*], Biao Yin [2], Yunchen Xiao [2], Gang Li [1] and Chuanliang Yan [3]

[1] Laboratory of Natural Gas Hydrate Extraction Technology and Comprehensive Utilization, Guangzhou Institute of Energy, Chinese Academy of Sciences, Guangzhou 510640, China
[2] School of Mechanical Engineering, Yangtze University, Jingzhou 434023, China
[3] School of Petroleum Engineering, China University of Petroleum (East China), Qingdao 266555, China
* Correspondence: dengfc@ms.giec.ac.cn

Abstract: Erosion wear is a common failure form of slotted screen in service. In this paper, based on CFD software and sand production data of a gas field in the Tarim Basin, the particle velocity and shear force at the slot of the flow field in the sieve tube were studied to determine the maximum area of erosion; at the same time, the velocity, viscosity, particle size and concentration of sand-carrying fluid were analyzed by orthogonal test, and the regression model of multi-factor maximum erosion rate was established. ① Through the analysis of the four factors on the degree of dependent variables, the order of the primary and secondary factors are: sand-carrying liquid flow rate, particle concentration, fluid viscosity, particle diameter, the effect of fluid viscosity and particle diameter on erosion rate is relatively small; ② According to the analysis of variance and range, the combination scheme of minimum erosion generation is obtained, and the calculation model of the erosion rate of the slotted screen is established. In order to reduce the erosion and abrasion in the actual oil and gas production process, the reasonable flow control and precise sand control method design and precision selection can be adopted; it provides a design basis for sand control and long-term effects of production in high-yield gas field.

Keywords: erosion wear; screen; CFD; orthogonal test; regression model

Citation: Deng, F.; Yin, B.; Xiao, Y.; Li, G.; Yan, C. Research on Erosion Wear of Slotted Screen Based on High Production Gas Field. *Processes* **2022**, *10*, 1640. https://doi.org/10.3390/pr10081640

Academic Editor: Farid B. Cortés

Received: 18 July 2022
Accepted: 13 August 2022
Published: 18 August 2022

1. Introduction

The gas field in the Tarim Basin is in the Paleoproterozoic Suwayi Formation and the Kumgremu Group. The area is a block bottom water anomalous high-pressure condensate reservoir which are low-porosity, low-permeability, fractured sandstone reservoirs. Since production began in 2009, high volume output has been maintained. However, as the field reached the middle and late stages of production, the sand output from gas wells increased and a significant drop in production occurred. A mechanical screen is used as the most common sand control tool in the process of a gas well, and is used to sort and block sand particles of different grain sizes. Due to its special working nature, erosion and wear often occur in its service process, making the screen's local effective wall thickness decrease, and the particles clog in the work, making the screen pressure-bearing capacity decrease, which eventually leads to the increase of well repair operations and also affects its service life and the opening rate of gas wells [1,2]. To ensure the production capacity as much as possible, therefore, the erosion life analysis of gas well screen has received more and more attention from scholars.

Initially, the study of screen erosion life was conducted by determining the erosion rate using the indoor hanging screen mass loss rate [3]. Later, Greene [4] used the CFD numerical modeling method to study the effect of annular flow rate on the erosion rate of the screen and established a semi-empirical erosion model. In China, Liu Yonghong [5] studied the influence law of various factors, such as erosion velocity, on the degree of erosion of cut-slit screen by using the method of indoor tests. Chen Bin [6] and others determined the

degree of influence of different external factors on the erosion rate through experiments in combination with the actual situation of offshore oilfield production. Scholars at home and abroad mainly use the erosion test device to simulate the erosion of screen specimens and establish the corresponding erosion prediction model [7]; some studies use computational fluid dynamics software to numerically simulate the erosion and wear of screen and analyze the influence of various factors on the erosion simulation of the screen on the basis of the verification of the selected erosion model, and mainly for the cut seam screen and wire-wound screen. Most of the studies are based on the simulated data only and do not discuss the turbulent changes in the internal flow field and the effect of particle motion on erosion. In this paper, based on the physical properties and production conditions of the on-site strata, a single-fracture flow field model of the flushed screen in the sand control production of gas wells is established. CFD-FLUENT is used to analyze and evaluate the screen erosion under different sensitive factors. The movement law of the internal flow field and the erosion and wear conditions will improve the selection basis of gas well erosion for sand control theory and parameters, and guide the production site.

2. On-Site Output Liquid Specimen Analysis

The study investigated the basic situation of the field and the data of the sand production, and found that its total number of wells is 30, the gas–oil ratio is 12,389 m^3/t, and the water–gas ratio is 0. Among them, wells, recorded mainly for the destination section except for the Su III section, have conglomerate or conglomerate-bearing silt-stone samples. This is shown in Figure 1, to understand the area out of the sand, which has basically full coverage. The sand samples were drawn from the anomalous wells with through-diameter tubing columns, and the particle size was generally larger than that of the wells with non-full through-diameter tubing columns. There were casing perforations of 8–12.8 mm, 3 mm perforations of the screen perforations, and the internal and external perforations were the same; the overflow area of its production screen was only 1/10 of that of the punching slit screen, and the sand particles were prone to clogging after entering the screen. The statistics showed that all gas wells in this block have different degrees of washout, and 56% of the wells are at the wellhead.

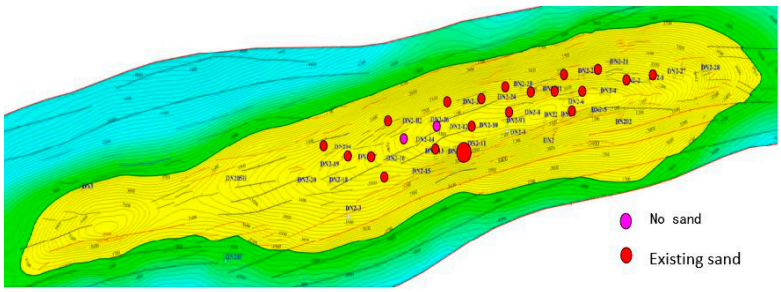

Figure 1. Sand production distribution of a gas field well in Tarim area.

As shown in Figure 2, sand samples were obtained by taking out the primary nozzle of a gas well. From the figure, the grain size goes up to 1 mm, while the particle cage sleeve erosion is serious, the orifice is basically linked, the individual orifice eye is inlaid with stones, and the bottom of the cage sleeve was eroded more seriously; the site cage sleeve plunger bottom can see a large area of erosion. The sand sample assays were used to obtain a silica-based skeleton of quartz particles and calcium carbonate cement.

Figure 2. Sand sample and erosion diagram of nozzle cage.

Figure 3 shows the monitored gas production versus oil pressure curve of a gas well in the block at different times, due to erosion damage making a blockage in the tubing. The blue solid line box in the figure shows the perforation time node—about one year between the two times. There is still a risk of pressure anomaly and well shutdown after unclogging the tubing column. Thus, as a downhole tool that directly contacts the formation and separates sand particles in gas wells, the punching seam screen is most prone to erosion and wear, and erosion research on screens has become inevitable to reduce the impact of screen failure on production capacity.

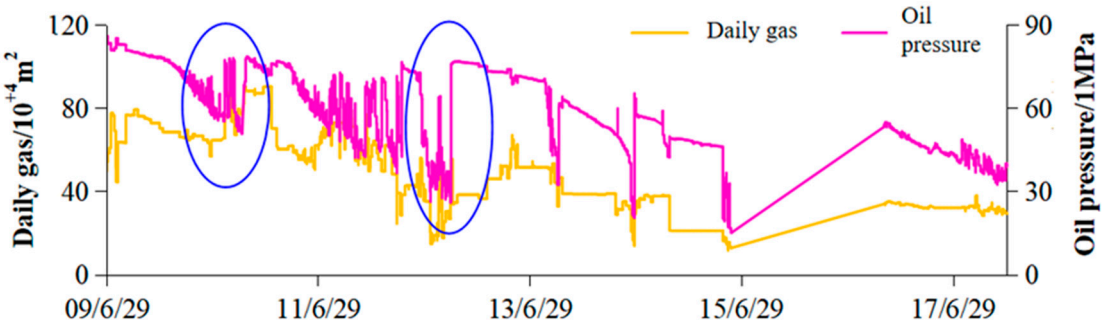

Figure 3. Relationship between gas production and oil pressure in a gas well at different times.

3. Mathematical Model of Erosion

3.1. Multiphase Flow Model

The process of high-speed airflow with sand eroding the screen is a complex gas-solid two-phase three-dimensional turbulent flow problem [8,9]. Given that the volume fraction of sand particles in the two-phase flow is relatively small (less than 10%). Therefore, the gas is treated as a continuous phase, and the gas control equation is adopted to describe the gas flow, while the sand particles are treated as discrete phases, and the Eulerian method is used to describe the main phase and the Lagrangian method to describe the discrete terms to track the motion process of the sand particles.

3.2. Control Equations

Under normal conditions of screen pressure, the sand-carrying motion of oil and gas is a complex turbulent process. K-ε turbulence model is the most widely used model in scientific research and engineering applications, and this model is suitable for turbulent flow with a high Reynolds number [10–12]. The continuity and momentum equations for continuous phase gas control are obtained from this model as follows:

$$\frac{\partial \rho}{\partial t} + \rho \frac{\partial u_j}{\partial x_j} = 0 \tag{1}$$

$$\frac{\partial u_i}{\partial t} + u_j \frac{\partial u_j}{\partial x_j} = \frac{1}{\rho} \frac{\partial p}{\partial x_i} + v \frac{\partial^2 u_i}{\partial xj^2} + f_i. \tag{2}$$

The equation for the forces acting on the discrete phase is obtained as [13]:

$$\frac{d\vec{u_p}}{dt} = \frac{\vec{u} - \vec{u_p}}{\tau_r} + \frac{(\rho_p - \rho)}{\rho_p} + \vec{F} \tag{3}$$

$$\tau_r = \frac{\rho_p d_p}{18\mu} \frac{24}{C_D \mathrm{Re}}, \tag{4}$$

where ρ is the fluid density (kg/m^3); u_i and u_j are the fluid flow velocities at different positions, m/s; p is the pressure (Pa); x_i and x_j are the two flow field coordinates; f_i is the mass force (N); $\vec{u}$ is the fluid phase flow velocity (m/s); $\vec{u_D}$ is the particle velocity (m/s); τ_r is the time required for the particle to reach thermal equilibrium (s); ρ_p is the particle density (kg/m^3); $\vec{F}$ is the additional acceleration term (N). μ is the fluid viscosity (mPa·s); d_p is the particle diameter (m); C_D is the particle concentration.

As we know, two different collision forces between particles and between particles and the wall act during the motion of particles. In the gas wells the inter-particle collision forces are negligible due to the small volume fraction of the particles [14]. Grant and Tabak off used mathematical analysis to obtain the sand-to-wall collision recovery coefficient (the effect of the collision force between the particles and the wall on the particle velocity) based on experiments as follows:

$$e_T = 0.993 - 1.76\alpha + 1.56\alpha^2 - 0.49\alpha^3 \tag{5}$$

$$e_T = 0.998 - 1.66\alpha + 2.11\alpha^2 - 0.67\alpha^3, \tag{6}$$

where e_T is the tangential recovery coefficient; e_N is the vertical recovery coefficient; α is the particle incidence angle (rad). The erosion rate is obtained as:

$$E = \sum_{1}^{n} \frac{m_i v^K}{A_f} f(\alpha), \tag{7}$$

where E characterizes the erosion rate (kg/(m^2·s)); m_i is the dimensionless particle mass fraction; V is the impact velocity, (m/s); K is the dimensionless velocity index; A_f is the erosion area (m^2); α is the impact angle (°).

3.3. Fluid Computing Area Establishment and Boundary Condition Setting

3.3.1. Model Establish

A slotted screen is generally used in the production process of oil fields with low mud content and a single reservoir [15]. The fluid calculation domain of the screen mainly considers the erosion effect of the sand-carrying fluid on the seam channel, and the simplicity and accuracy of the calculation. The fluid domain model is established without considering the length of the entire flow channel. A suitable seam width is invoked as the model of the screen of the sand control column of the punching slit tube. In this study, a single runner model of the punching seam sleeve was intercepted, the seam length was 18 mm, the seam width was 0.4 mm, and the runner width was 3 mm divided into hexahedral structured meshes by ICEM, and the mesh was refined for local areas, and a total of 367,659 cells and 345,220 nodes were obtained after verifying the grid independence. The wall surface is N80 material. The upper part of the model is the fluid inlet, and the two seam way outlets are located in the lower part. The mesh area with a large pressure gradient is defined by local encryption to obtain the solid and flow channel mesh model of the punching slit screen as shown in Figure 4.

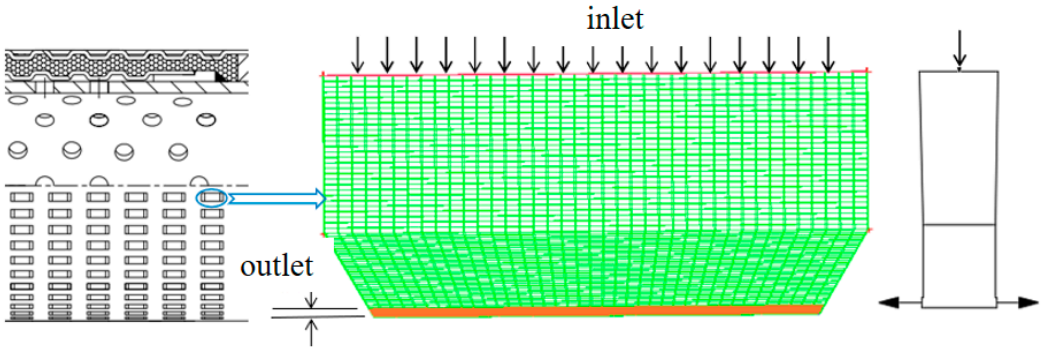

Figure 4. Schematic diagram of flow channel grid of single slit screen.

3.3.2. Boundary Conditions

According to servicing punching slit screen working conditions on the oilfield, different specific parameters, such as sand carrying fluid velocity, sand concentration and particle diameter, are selected and numerical simulation analysis is carried out according to the working conditions shown in Table 1. Since the flow rate of compressible gas is not too large under high pressure, the initial boundary conditions are set as flow rate 4 m/s, fluid viscosity 0.03 mPa·s, particle diameter 0.4 mm (normal distribution) and particle concentration 3%. The erosion calculation uses the Realizable k-ε turbulence model, and the wall is set with a suitable rebound coefficient. The velocity-pressure in-let is used for the inlet, while the particle injection surface is set. Pressure outlet boundary conditions are employed to the outlet. The discretization of momentum, kinetic energy, turbulent kinetic energy and turbulent dissipation rate is in second-order windward format, and the SIMPLE algorithm is used for pressure-velocity coupling.

Table 1. Simulation scheme of influencing factors.

Influencing Factors	Initial Simulated Value	Comparative Simulation Condition
velocity/(m/s)	4	2, 3, 4, 5, 6
viscosity/(mPa·s)	0.03	0.01, 0.03, 0.05, 0.07, 0.09
Particle size/(mm)	0.3	0.2, 0.3, 0.4, 0.5, 0.6
Particle concentration	3%	1%, 3%, 5%, 7%, 9%

3.3.3. Internal Flow Field Analysis

The magnitude of the wall shear force can be used to characterize the risk of erosion wear of the pipeline [16]. Figure 5a shows the flow field velocity vector diagram of the particles in the screen tube under the initial working condition. When the sand particles flow into the screen gap, the overall trend is to move in the direction of the sand inlet velocity. The sand particles tend to move towards the outlet of the flow channel, and the sand particles near the outlet have higher velocity than other parts of the inner flow field. Figure 5b is a scatter diagram of the wall shear force at different node coordinates along the *z*-axis of the screen tube, in which the two outlets of the screen tube show a high wall shear force, with a maximum of 6.45×10^4 Passcal appearing at the outlet. In the upper part (the upper end of the yellow dashed box in Figure 5b), the fluid turbulence at the outlet of the punching sleeve is relatively severe, and the fluid shear force is large. In the flow field in the punching sleeve, the farther away from the outlet, the smaller the turbulent kinetic energy (blue dotted line area).

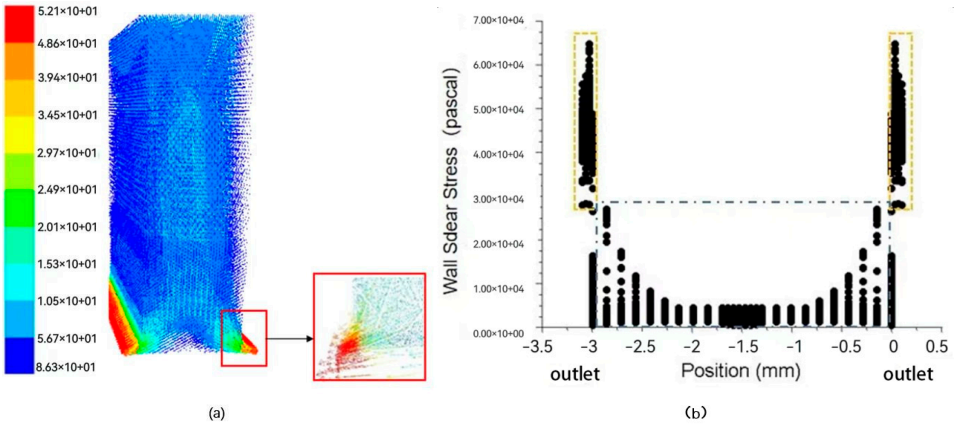

Figure 5. Particle velocity vector diagram of flow field in screen (**a**) and a scatter diagram of wall shear force along Z axis of screen (**b**).

3.4. GasWell Screen Erosion Law Study

Figure 6a shows the trajectory of the particles flowing into the screen, which shows that the force is the principal influence on the particle motion. After stabilization of the flowing fluid, the particles will flow out from the outlet directly under the action of the fluid traction. The erosion rate, as an important parameter for evaluating the erosion layer degree, expresses the amount of loss per second per unit screen wall. Figure 6b shows the erosion rate cloud of the screen (the right side is the cloud of the bottom of the screen), the sand particles at the entrance of the flow channel reaches its maximum, the erosion rate at both sides of the bottom, that is, at the exit of the flow channel, is the largest (red circular realization box) is 5.69×10^{-5} kg/(m^2·s). At this time, the sand-containing oil and gas have the most serious erosion and wear on the screen gap, and the analysis results are consistent with the analysis of erosion and wear from the perspective of the wall shear force.

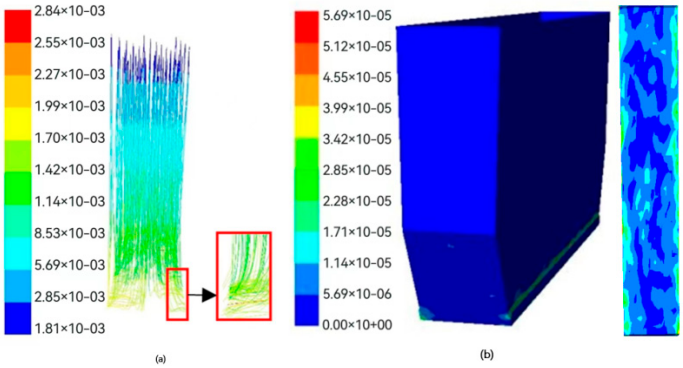

Figure 6. Particle trajectory diagram (**a**) and the erosion rate contour of screen (**b**).

Figure 7a shows the scatter plot of turbulent kinetic energy distribution of the flow field in the screen at different positions along the *z*-axis, from which it can be concluded that the total turbulent energy at the outlet of the screen is larger, and the more to the middle of the step surface of the screen, the smaller the turbulent kinetic energy obtained. The results further verify the results of wall shear distribution in Figure 5b. Figure 7b shows the particle velocity cloud at the exit of the screen, and it can be seen that the velocity of the particles is greater when they are on both sides near the exit step surface compared to the middle. In addition, by comparing the results of flow field analysis in the screen, it can be concluded that the higher the turbulent kinetic energy of the fluid and wall shear force against the exit, resulting in the higher particle velocity at the exit, the more obvious the erosion effect of the screen around the exit, which is consistent with the erosion cloud diagram of the screen. For the more serious gas wells in sanding, the sand and calcium

will be higher, the greater the number of particles impacted on the screen per unit area, resulting in a much higher erosion rate, which is more harmful to the screen sand control.

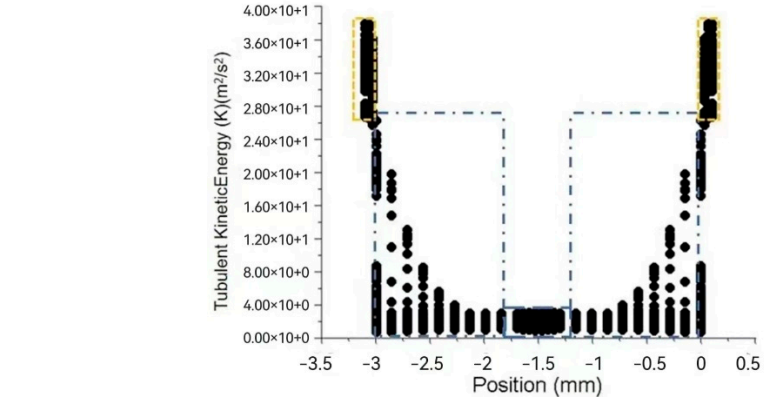

(**a**)

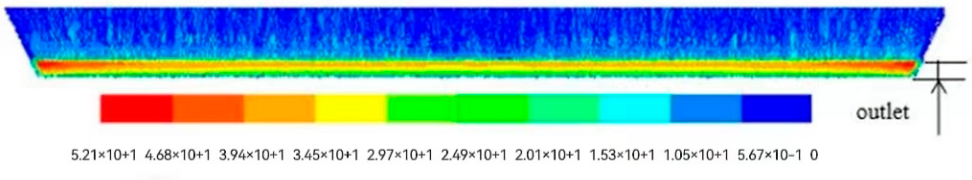

(**b**)

Figure 7. (**a**) Scatter diagram of Turbulent kinetic energy along Z axis of screen. (**b**) Contour of particle velocity at screen outlet.

4. Erosion Influence Law Study

4.1. Effect of Different Factors on the Erosion Rate of Screen

According to the field sample of this gas field and the specific working environment of the punching slit screen combined with the above equation, the sensitive factors of the erosion rate, including velocity (A) and viscosity (B), particle diameter (C) and particle concentration (D), are defined as variables. The study formulated the following orthogonal analysis table simulation scheme (Table 2) to predict the degree of influence of several different sensitive factors on the evaluation index and quantitatively calculate the maximum erosion rate in the tube, taking five level values for each factor and conducting orthogonal tests according to the table developed in orthogonal table $L_{25}(5^6)$.

We use the above data to conduct a static analysis of the average value of water for each factor, while determining that there is not any interaction between the factors, to obtain the mean response of each factor (Table 3). From the value of Delta in the table (for the detection of changes in the mean value, the larger the value, the more obvious the impact on the dependent variable) can be obtained for each factor on the screen erosion of the degree of the influence of the order: A > D > B > C.

The analysis of extreme variance (ANOVA) is widely used to analyze the comparison of the degree of influence of multiple factors. However, whether the effect of the dependent variable is significant or not needs the introduction of an analysis of variance of the original data [17]. The F-value is the ratio of the two means; a larger F represents more significant differences between groups. The *p*-value is the judgment indicator; the *p* value of the flow rate is less than 0.05, then the null hypothesis can be rejected. Based on the results, it was determined that there was a significant effect of flow velocity size on the erosion rate, a reliable effect of particle concentration, and no significant effect of changes in viscosity and particle size on the erosion rate.

Table 2. Orthogonal test scheme.

Velocity (m/s)	Viscosity (mPa·s)	Particle Diameter (mm)	Particle Concentration (%)	Maximum Erosion Rate /10^{-5} kg/(m^2·s)
2	0.01	0.2	1	1.38
2	0.02	0.3	3	3.39
2	0.03	0.4	5	4.46
2	0.04	0.5	7	4.82
2	0.05	0.6	9	5.76
3	0.02	0.2	7	21.6
3	0.03	0.3	9	23.8
3	0.04	0.4	1	2.36
3	0.05	0.5	3	6.68
3	0.01	0.6	5	16.5
4	0.03	0.2	3	26.5
4	0.04	0.3	5	42
4	0.05	0.4	7	52.3
4	0.01	0.5	9	117
4	0.02	0.6	1	9.08
5	0.04	0.2	9	86.7
5	0.05	0.3	1	8.39
5	0.01	0.4	3	30.8
5	0.02	0.5	5	101
5	0.03	0.6	7	136.3
6	0.05	0.2	5	166
6	0.01	0.3	7	261
6	0.02	0.4	9	334
6	0.03	0.5	1	56
6	0.04	0.6	3	103

Table 3. Mean response table of influencing factors.

Lever	A (m/s)	B (mPa·s)	C (mm)	D (%)
1	3.962	85.336	60.436	11.162
2	14.188	93.814	67.716	34.074
3	49.376	45.132	84.784	65.992
4	72.638	47.776	52.820	95.204
5	179.720	47.826	54.128	113.45
Delta	175.758	48.682	31.964	102.29
F-Value	7.74	0.87	0.27	2.78
p-Value	0.007	0.521	0.891	0.102

4.2. Establishment of the Erosion Regression Model

The analysis was based on the data in the orthogonal scheme design, and then after normalizing the data to de-quantitative, the least squares method was used to obtain the model parameters using MATLAB, and it was determined that there was no interactivity relationship between the factors. Thus, the maximum erosion rate fitting model was obtained as:

$$E_r = 4040v^2 - 140v - 1200\mu - 120|d - 0.3| + 2400c + 230, \quad (8)$$

where: v is the flow rate of sand fluid carried by the screen (m/s), μ is the fluid viscosity (mPa·s), d is the particle size (mm), and c is the particle concentration.

The orthogonal test table can get the main effect. Figure 8a shows that with the sand carrying liquid flow rate and particle concentration increase the erosion rate will also increase, with a particle size of0.4 mm, erosion reached the maximum. That is, the

slit width is to get the minimum erosion rate of the screen. There is a combination of factors in the flow rate of 2 m/s, fluid viscosity 0.03 mPas, particle size 0.3 mm and particle concentration of 1% to meet the minimum erosion rate. Based on the maximum erosion rate data from the orthogonal test in Table 2, the values of the four independent variables enter into Equation (8), and the results compared with the fitting function are shown in Figure 8b below. The coefficient of determination R^2 = 0.843 for the adjusted fitted equation can be obtained by comparing Table 2. The study calculated the model error rate of 9.2%, which inferred that the fitted equation has some accuracy.

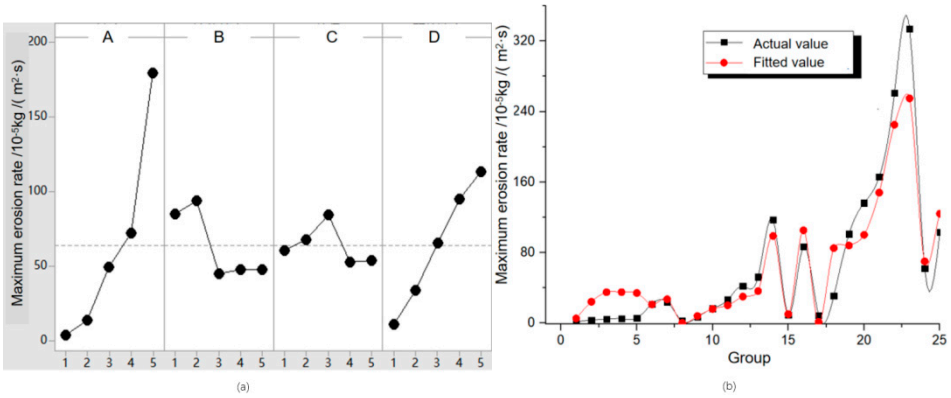

Figure 8. Main effect diagram (**a**) and regression equation data comparison diagram (**b**).

According to the data of the perforated screen in service in the gas field of this block, a three-dimensional model is established, and the boundary conditions are set according to the parameters of 2 m/s, fluid viscosity 0.03 mPa·s, particle size 0.3 mm, and particle concentration of 1% when the punching seam sieve produces the minimum erosion rate [18]. Since the maximum erosion rate of the perforated screen is 1.02 × 10^{-5} kg/(m^2·s), the simulation results in Figure 9 shows that the perforated screen used in this high production gas field has a greater erosion rate under the same conditions. The result shows that the punching slit screen has lower erosion, longer life and better sand control compared to the perforated screen.

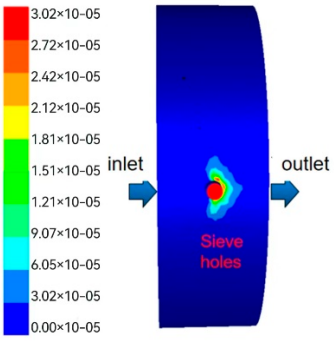

Figure 9. The contour of erosion rate in perforated screen.

Combined with the actual working conditions of the fluted screen in high-yield gas wells, it is concluded that in order to reduce the impact of screen erosion and wear on oil and gas production, the flow rate of the sand-carrying fluid can be properly controlled under the condition of meeting the normal production requirements, and as and control method can be reasonably designed to reduce the sand content in the produced fluid, thereby reducing the particle concentration of the fluid passing through the screen gap. [19] At the same time, the selection principle of sand control design is also put forward to avoid the occurrence of the situation that the median sand particle size in the formation is equal

to or similar to the screen crack width, which has guiding significance for actual oil and gas exploitation.

5. Conclusions

1. Numerical simulation is used to simulate the results of particle and fluid movement in the flow field of the screen in combination with the actual sand output data of the gas wells in the field. The causes and results of different erosion rates in different parts of the screen are studied and analyzed. In order to effectively ensure the service life of the screen, a pre-protective coating can be applied to the area with a high erosion degree for local protection.

2. The orthogonal tests were synthesized and quantitatively calculated to summarize several different sensitive factors on the erosion law of the screen, and listed in their primary and secondary order. The results revealed that the flow rate of sand carrying liquid and the size of sand concentration are the main causes of erosion and wear. Only for reasonable control of each factor can there be a guiding role in the stable production of the screen size.

3. By processing the proposed orthogonal analysis data through the established DPM model, the fitted relationship equation between the screen erosion rate and different factors is established, and the influence law on the screen erosion is obtained. It provides an effective means to mitigate the effect of blockage inside the screen due to erosion and abrasion of the screen in the actual working process of high production gas wells. It is a better solution to reduce the workload and cost.

Author Contributions: Conceptualization, F.D. and G.L.; methodology, F.D.; validation, F.D. and C.Y.; formal analysis, B.Y.; data curation, C.Y.; writing—original draft preparation, B.Y. and Y.X.; writing—review and editing, F.D.; supervision, F.D. All authors have read and agreed to the published version of the manuscript.

Funding: This research was funded by National Science and Technology Major Special Project (2016ZX05025-002-003); National Science and Technology Major Project (2016ZX05022006-004); the Special Project for Marine Economy Development of Guangdong Province(GDME-2020D044); Hubei Provincial Technical Innovation Special Project (2016ACA181).

Institutional Review Board Statement: Not applicable.

Informed Consent Statement: Not applicable.

Data Availability Statement: Not applicable.

Conflicts of Interest: The authors declare no conflict of interest.

References

1. Yang, Y.; Xie, W.; Zhang, J.; Guo, C.; Wang, X. Distribution characteristics and detection of leakage magnetic field in defect shape of inner wall of natural gas. *Transducer Microsyst. Technol.* **2020**, *39*, 104–107.
2. Wang, K.; Li, X.F. Numerical Prediction of the Maximum Erosion Location in Liquid-Solid Two-Phase Flow of the Elbow. *J. Eng. Thermophys.* **2014**, *35*, 691–694.
3. Liu, Z.; Han, B.; Zhang, K. Erosion test device of the sand management for oil and gas well. *Hydraul. Pneum. Seals* **2015**, *35*, 35–38.
4. Greene, R.M.; Moen, T. The impact of annular flows on high rate completions. In Proceedings of the SPE International Symposium and Exhibition on Formation Damage Control, Lafayette, LA, USA, 15–17 February 2011.
5. Liu, Y.; Zhang, J.; Ma, J.; Li, X.P. Erosion Wear Behavior of Slotted Screen Liner for Sand Control. *Tribology* **2009**, *29*, 283–287.
6. Chen, B.; Zhang, Q.; Gong, N. Experimental Study on Erosion Wear of Sand Control Composite Screen in Water Source Well. *China Pet. Mach.* **2019**, *47*, 93–100.
7. Chen, D.; Zhang, E.; Shuanggui, L.I.; Dandan, L.I.; Zhu, H.; Zeng, D. Analyses of Anti-erosion Performance of Drilling Crossunder Emergent Discharge Conditions. *Corros. Prot.* **2018**, *39*, 698–703, 732.
8. Wang, Z.; Xu, L.; Yan, Y.; Li, S.; Zhang, J.; Sun, L.; Cao, M. Numerical simulation of the erosion due to particles within bypass crossover sub in the fracturing process of horizontal wells under eccentric working conditions. *J. Northeast. Pet. Univ.* **2020**, *44*, 98–106, 111.
9. Deng, F.; Deng, J.; Hu, L.; Yu, B.; Tan, Q.; Xu, Y. Simulation research on the erosion of slotted screen for the unconsolidated sand formation. *Arab. J. Sci. Eng.* **2014**, *39*, 5237–5243.

10. Zhang, R.; Hao, S.; Yu, Y. Simulation Experiment of Erosion of Sand Control Screen in Deep Water Gas Well Based on CFD. *Res. Explor. Lab.* **2019**, *38*, 73–77, 82.
11. Wang, S. *Study on Erosion and Structure Optimization of Nozzle for Oil and Gas Well*; Xi'an Shiyou University: Xi'an, China, 2018.
12. Sun, Y.; Lou, Y.; Cao, Y.; Wen, M.; Zhai, X.; Zhao, X. Numerical simulation of the erosion process of wire wrapped screen based on erosion-dynamic grid coupling. *Oil Drill. Prod. Technol.* **2021**, *43*, 160–169, 238.
13. Zhanghua, L.; Chen, X.; Lin, T.; Ming, X.; Zheng, J. Study on Erosion Mechanism of Bending Joint in Blooey Line. *J. Southwest Pet. Univ.* **2014**, *36*, 150–156.
14. Wang, Y.; Xing, H.; Zhang, L. Experimental on Performance Evaluation of Foam Metal Sand Control Screen. *China Pet. Mach.* **2019**, *47*, 90–97.
15. Zhang, X.; Martin; Wang, D.; Yan, J.; Zhang, B.; Zhang, Y.; Chen, G. Development and Application of High-strength Erosion-resistant Sieve Pipe for Hot Mining in Horizontal Well. *China Pet. Mach.* **2015**, *43*, 90–92.
16. Li, J.; Yao, C.; Li, X. Numerical Simulation Investigation on erosion of Oil Pipeline. *Technol. Dev. Chem. Ind.* **2016**, *45*, 66–68.
17. Jiang, Z.; Huang, X.; Xiong, Y.; Zeng, Y. Optimization of Multi-point Progressive Forming Process for Sheet Based on Orthogonal Test and BP Neural Network. *Forg* **2015**, *40*, 33–37.
18. Deng, F.; Huang, B.; Yin, B.; Li, X.; Yi, X. Research on the erosion of punched casing in natural gas hydrate exploitation. *J. Cent. South Univ.* **2022**, *53*, 1023–1032.
19. Yin, B.; Deng, F.; Shen, X.; Chen, S.; Wen, M. Simulation study on fouling rate of punched screen. *China Saf. Prod. Sci. Technol.* **2021**, *17*, 120–125.